online data

Interactive domains between pore loops of the yeast K^+ channel TOK1 associate with extracellular K^+ sensitivity

Ingela JOHANSSON and Michael R. BLATT[1]

Laboratory of Plant Physiology and Biophysics, IBLS - Plant Sciences, Bower Building, University of Glasgow, Glasgow G12 8QQ, U.K.

Gating of the outward-rectifying K^+ channel TOK1 of *Saccharomyces cerevisiae* is controlled by membrane voltage and extracellular K^+ concentration. Previous studies identified two kinetically distinct effects of K^+, and site-mutagenic analysis associated these K^+-dependencies with domains of the extracellular turrets of the channel protein. We have mapped the TOK1 pore domains to extant K^+ channel crystal structures to target additional residues contributing to TOK1 gating. Leu^{270}, located in the first pore domain of TOK1, was found to be critical for gating and its K^+ sensitivity. Analysis of amino acid substitutions indicated that spatial position of the polypeptide backbone is a primary factor determining gating sensitivity to K^+. The strongest effects, with L270Y, L270F and L270W, led to more than a 30-fold decrease in apparent K^+ affinity and an inversion in the apparent K^+-dependence of voltage-dependent gating compared with the wild-type current. A partial rescue of wild-type gating was obtained on substitution in the second pore domain with the double mutant L270D/A428Y. These, and additional results, demarcate extracellular domains that are associated with the K^+-sensitivity of TOK1 and they offer primary evidence for a synergy in gating between the two pore domains of TOK1, demonstrating an unexpected degree of long-distance interaction across the mouth of the K^+ channel.

Key words: cation selectivity gating, outward-rectifying potassium channel, protein domain interaction, *Saccharomyces cerevisiae*, voltage- and potassium-dependent channel gating.

INTRODUCTION

Voltage-gated K^+ channels incorporate at least seven major evolutionary families, including the Kv (voltage-gated K^+ channel) family, that are constructed around a core of six transmembrane α-helices (the so-called S1–S6 helices), a P loop and helix that contribute to the channel pore and ion-selectivity filter, and a voltage sensor that is associated with the S1–S4 helix complex [1]. The complex of P loop and helix, and the flanking transmembrane helices are also common to the inwardly (Kir) and weakly rectifying K^+ channels that comprise only two membrane-spanning α-helices, designated M1 and M2, and to the so-called double- or two-pore (domain) K^+ channels that appear to have arisen by gene duplication and fusion of two Kir coding sequences (e.g. TWIK [2] and KCO1 [3]).

Crystal structure analyses have indicated a remarkable degree of similarity between these K^+ channel families and across phylogenetic boundaries [4–8]. In each case, positioned around the pore of the functional K^+ channel is a tetramer of peptide domains: the channel pore itself is lined by four inner helices (the Kv S6 helix or the Kir M2 helix), one from each polypeptide subunit, that lie substantially off the normal to the plane of the membrane and form a 'diaphragm' or inverted 'teepee'-like arrangement to narrow the pore near the inner membrane surface. Opening of the pore is thought to depend on a proline (PXP) or glycine 'hinge' domain within the inner (S6 or M2) helix and its rotation, coupled to movement of the outer (S5 or M1) helix, draws apart the pore diaphragm. For Kv channels that are activated by depolarization, this gating movement couples to voltage by a semi-co-operative [9,10] outward-directed displacement of the positively charged S4 helix in each subunit which tugs on the S4–S5 linkage, located near the inner face of the membrane, thereby drawing open the S6 diaphragm [5,11]. The same principle appears to work in reverse for Kv-type channels that activate on hyperpolarization (i.e. opening of the S6 diaphragm is coupled to inward-directed movement of the S4 helix) in cardiac HCN [12] and bacterial MVP K^+ channels [13] and the KAT1 K^+ channel in *Arabidopsis* [14].

One subset of K^+ channels separate from this norm. Gating of several outward-rectifying K^+ channels in plants and fungi is coupled both to voltage and to extracellular K^+. These channels open on membrane depolarization to facilitate K^+ flux out of the cell; however, uniquely, they do so only at membrane voltages positive of the K^+ equilibrium potential, E_K, ensuring that the channels are closed under conditions where the K^+ gradient is directed inward while retaining the ability to release K^+ over a wide range of K^+ concentrations. TOK1 (also called YKC1, DUK1 or YORK), the outward-rectifying K^+ channel of the *Saccharomyces cerevisiae* plasma membrane, is a case in point. The TOK1 K^+ channel is activated by membrane depolarization [15,16] and, additionally, its opening is suppressed by increasing extracellular K^+ above approx. 1–3 mM [15,17,18], resulting in a positive shift in the current–voltage (IV) curve in parallel with E_K. These characteristics are retained when the channel is expressed heterologously, indicating that its sensitivity to K^+ is intrinsic to the channel protein.

How is this K^+-sensitivity achieved? TOK1 has an unusual structure of two pore loops and eight transmembrane domains, as if it originated from the fusion of one element each of Kv and Kir channel proteins. The first pore domain (P1) comprises transmembrane helices S5 and S6 and the second pore domain (P2) is formed by transmembrane helices S7 and S8 [15]. Both pore domains contribute to gating as well as permeation [17,19,20], although they are not functionally equivalent

Abbreviations used: E_K, K^+ equilibrium potential; E_{rev}, tail current reversal voltage; $[K^+]_o$, external K^+ concentration; Kir, inwardly rectifying K^+ channel; Kv, voltage-gated K^+ channel; MthK, *Methanobacterium thermoautotrophicum* K^+ channel; SKOR, stelar K^+ outward rectifying.

[1] To whom correspondence should be addressed (email m.blatt@bio.gla.ac.uk).

[19,21]. The observation that K^+ at submillimolar and millimolar concentrations had different effects on the gating of TOK1 led Vergani et al. [19] to propose the existence of two binding sites for K^+, one each associated with the high- and low-affinity gating responses. Site mutations at two pairs of amino acid residues on the extracellular face of P1 and P2 were identified to affect the K^+-sensitivity of gating, raising a question about localized binding pockets in the outer mouth of the pore, either close to [19,21] or within [22] the selectivity filter of the pore itself. Nonetheless, the identity of these sites, their co-operativity between pore domains and their relationship to binding in the permeation pathway has yet to be explored.

We have taken advantage of recent crystallographic data [4,6,8,23] to identify sites associated with these putative K^+-binding domains. In the present paper, we report that substitutions at one site especially, Leu^{270} in P1, dramatically alters the K^+-sensitivity of TOK1. Remarkably, mutation at this site partially rescues the effects of substitution at a second critical site in the adjacent pore loop. These results support the proposed extracellular K^+ binding pockets on the TOK1 surface; furthermore they offer primary evidence for long-distance interactions between pore domains of this unusual K^+ channel.

MATERIALS AND METHODS

Molecular biology

The plasmid pEXTM1 containing the coding region of *TOK1*, cloned into the BalI/StuI sites and flanked by the 3′- and 5′-untranslated sequences of the *Xenopus* β-globin gene [18] was used as a template for site-directed mutagenesis and expression. Site-directed mutagenesis was carried out using a recombinant PCR technique [24] with primers containing the desired mutation. Double mutants were constructed by ligating the BstXI fragment containing A428Y into previously mutagenized plasmids (containing L270D or L270Y). All mutants were verified by sequencing. Plasmids were linearized using HindIII and capped cRNA was synthesized *in vitro* using an mMessage mMachine kit (Ambion). cRNA was purified and diluted to 1 ng/nl in RNase-free water.

Oocyte preparation and injection

Stage V and VI oocytes were isolated from mature *Xenopus laevis* and were injected with 10–50 nl of cRNA (1 ng/nl) after partial digestion of the follicular cell layer with 2 mg/ml collagenase (type 1A, Sigma) for 1 h. Injected oocytes were incubated in ND96 (96 mM NaCl, 2 mM KCl, 1 mM $MgCl_2$, 1 mM $CaCl_2$ and 10 mM Hepes/NaOH, pH 7.4) supplemented with gentamycin (0.1 mg/ml) at 18 °C for 3 days before electrophysiological recordings.

Electrophysiology

Whole-cell currents were recorded under voltage clamp using an Axoclamp 2B (Axon Instruments) two-electrode clamp circuit and virtual ground. Microprocessor interface was via a LAB/LAN analogue/digital interface and software (Y-Science at http://www.gla.ac.uk/ibls/BMB/mrb/lppbh.htm). Intracellular electrodes were filled with 3 M KCl. Connection to the amplifier headstages were via a 3 M KCl Ag/AgCl half-cell, and matching half-cells with 3 M KCl agar bridges were used for connection to the virtual ground. Measurements were carried out under continuous perfusion at room temperature (20 °C). The bath solution consisted of 10 mM Hepes/$Ca(OH)_2$, pH 7.4, 1 mM $MgCl_2$, 100 mM sorbitol and 100 mM KCl and NaCl. For selectivity measurements, 100 mM KCl and NaCl were replaced by 30 mM KCl, RbCl, CsCl or NaCl and 70 mM *N*-methylglucamine chloride.

RESULTS

Current through TOK1 is composed of three kinetically distinct components [19]: an instantaneous component which appears within 1–2 ms of the onset of a depolarizing voltage step, a fast component ($t_{1/2} \approx 0.5$ s) and a slow component ($t_{1/2} \approx 30$ s). The distribution of current between each of these kinetic components is affected by the $[K^+]_o$ (external K^+ concentration) as well as by the voltage. Notably, the slow component is suppressed as K^+ outside rises from submillimolar to millimolar concentrations such that, for $[K^+]_o$ above approx. 10 mM, the fast component dominates and the slow component is virtually absent (see Figure 2, and also Figure 1 of [19]). Above 3 mM, increasing $[K^+]_o$ also suppresses TOK1 current and conductance at any one voltage so that the current–voltage (IV) and conductance–voltage (GV) curves shift roughly in parallel with E_K [15,17,18]. These characteristics define a minimum model for gating comprising a linear series of three closed states (C_2–C_4) that communicate with the open state (O_1) of the channel as $C_4 \leftrightarrow C_3 \leftrightarrow C_2 \leftrightarrow O_1$, consistent with the three distinct kinetic components to the current. Of these, the transition between the open state and the neighbouring closed state (C_2) must be extremely rapid ($t_{1/2} < 1$–2 ms) and voltage-dependent to account for the substantial, near-instantaneous component of the current on depolarization [17,22]; in turn, the more distal transitions, $C_2 \leftrightarrow C_3$ and $C_3 \leftrightarrow C_4$, accommodate the fast- ($t_{1/2} \approx 1$ s) and slow-relaxing ($t_{1/2} > 10$ s) components [17,19].

Within this scheme, the dual effect of K^+ was interpreted previously in the context of two binding sites for K^+, one high-affinity and one low-affinity site [19,21]. Furthermore, previous work from this laboratory [19,21] identified two sets of amino acid residues that are associated with corresponding sequences in each pore domain that, when mutated, affected one or both of these K^+-sensitive gating responses. Mutations of Leu^{293} (P1) and Ala^{428} (P2), C-terminal of the selectivity filter sequences G(Y/L)GD (see Figure 1), affected the balance between slow- and fast-kinetic components (a high-affinity response; apparent $K_{1/2} \approx 1$ mM K^+) as well as shifting the voltage-dependence of the current and conductance (a low-affinity response; apparent $K_{1/2} > 10$ mM K^+) [19]; mutations of residues Asn^{276} (the previous designation of Asn^{276} as Asn^{275} [21] is incorrect) (P1) and Asn^{410} (P2) were found to affect only the balance between slow- and fast-kinetic components [21].

The kinetic differences in these responses, and their alliance with different sequence domains adjacent to the pore loops, led us to revisit their possible association with two distinct K^+-binding pockets near the mouth of the channel pore. We mapped the sequences of the two pore domains of TOK1 to the crystal structures of the bacterial KcsA, MthK (*Methanobacterium thermoautotrophicum* K^+ channel), KvAP and Kv1.2 K^+ channels [5,6,8,23], and used the residues known to affect the K^+-sensitivity of TOK1 gating as starting points in our search. This analysis (see the Discussion) indicated two sets of putative co-ordination sites formed between the two extracellular loops either side of each pore loop and helix, that is between the S5–pore helix linker and the pore loop–S6 linker for P1 and between the S7–pore helix linker and the pore loop–S8 linker for P2. We identified two key sets of residues, Leu^{270} and His^{271} in P1 and Glu^{404} and Asn^{405} in P2, that are situated between the two putative co-ordination pockets (Figure 1), for site-directed mutagenesis and subsequent analysis after expression in *Xenopus* oocytes.

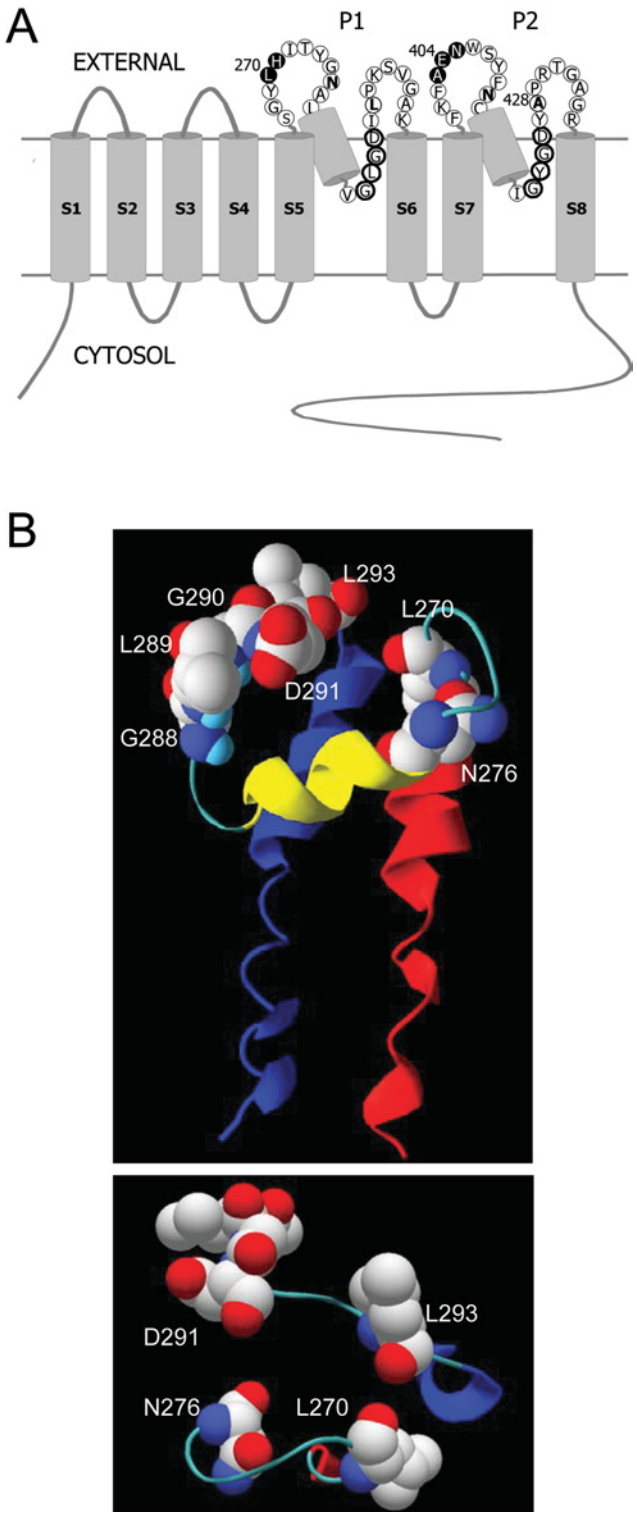

Figure 1 Structure of TOK1

(**A**) Topological model of TOK1 showing the sequences for the two pore loops, P1 and P2. Amino acid residues that were selected for substitution (Leu^{270}, His^{271}, Ala^{403}, Glu^{404} and Asn^{405}) are shown in reverse typeface. Ala^{428} was shown previously to be important for K^+ sensing [19] and was mutated in the double mutants characterized in the present paper. The selectivity filters (GLGD in P1 and GYGD in P2) are indicated in bold circles. (**B**) Model of pore domain P1 of TOK1 showing the position of Leu^{270} based on mapping to the crystal structure of MthK [23]. The channel pore structure is shown from the side (above) with the intracellular solution at the bottom and in slab view from the outside (below). Leu^{270}, Asn^{276}, Asn^{293} and the GLGD selectivity filter sequence are shown in space-filling representation.

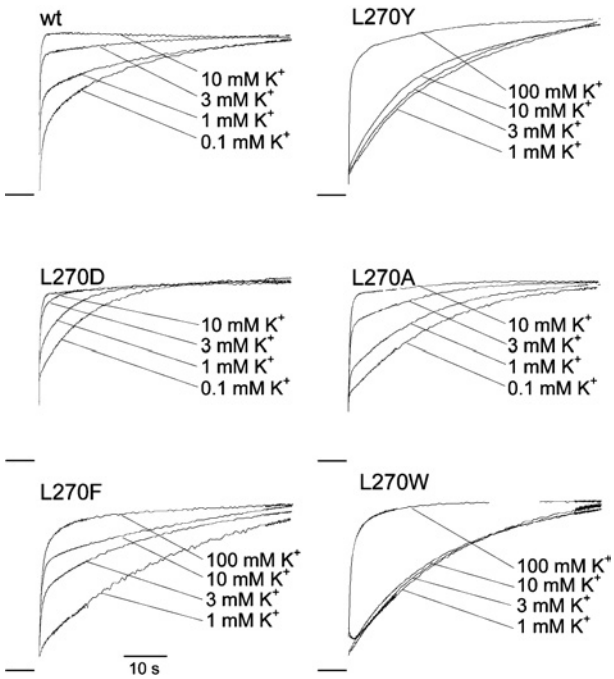

Figure 2 Mutations of Leu^{270} affect the activation kinetics of TOK1

Representative current traces from oocytes injected with wild-type (wt), L270Y, L270D, L270A, L270F and L270W cRNA, recorded in different concentrations of external K^+ as indicated. Holding voltage, −120 mV; test voltage, +30 mV. Currents are normalized to the estimated current maximum. The zero current level is indicated to the left of each set of traces. Scale bar, 10 s.

Mutations constructed for the sites in P2 proved uninformative (see the Supplementary Table at http://www.BiochemJ.org/bj/393/bj3930645add.htm). Even the most conservative substitutions in this pore domain, including E404Q and E404D, failed to give functional channels. At the adjacent position, neither A403D nor A403K produced functional channels, but the more conservative mutations of A403C and A403S yielded TOK1 currents with activation kinetics and voltage-dependencies that did not differ significantly from the wild-type (results not shown). Similarly, substitutions of aspartate, lysine and tyrosine for Asn^{405} were indistinguishable from the wild-type, both in the current kinetics and voltage-dependence (results not shown). The failure to produce functional mutants of Glu^{404} suggested an important role for this site in the function of the channel.

Leu^{270} in P1 is crucial to the K^+-sensitivity of current activation

In contrast, we successfully recovered substitutions in P1 with profound effects on TOK1 gating. Figure 2 shows current trajectories for wild-type TOK1 and several Leu^{270} mutants recorded from oocytes bathed in external K^+ concentrations between 0.1 and 100 mM. In each case, TOK1 current was activated with positive voltage steps to +30 mV for 60 s from a holding potential of −120 mV. As before [19,21], activation of wild-type TOK1 current was characterized by three kinetically distinct components, with increasing $[K^+]_o$ favouring the instantaneous and fast-kinetic components at the expense of the slow-relaxing ($t_{1/2} > 10$ s) component. A qualitatively similar pattern emerged for the Leu^{270} mutants. Quantitatively, however, the sensitivity to $[K^+]_o$ was visibly altered, dramatically so for several of the mutants. Substitution of tyrosine for Leu^{270} showed a profound slowing of current activation at all K^+ concentrations tested such that, even in 100 mM K^+, a significant slow-relaxing component

to the current was still evident. Similarly extreme effects were observed for the L270W mutant and, to lesser extents, for L270F, L270D and L270A. In every case, appreciably higher concentrations of K^+ were required to recover activation kinetics similar to those of the wild-type current.

To quantify and compare the effects of mutations on the current kinetics, we fitted the current traces, including those in Figure 2, to a sum of exponential functions as

$$I = a_i + a_f\left(1 - e^{-k_f t}\right) + a_s\left(1 - e^{-k_s t}\right) \quad (1)$$

where a_i, a_f, a_s are the amplitudes of the instantaneous, fast and slow components respectively, and k_f and k_s are the corresponding relaxation constants. The amplitudes derived from the fittings were used to obtain the fractional amplitude of current in the fast-kinetic component f_a [$= a_f/(a_f + a_s)$; see Figure 3A]. As expected from a visual inspection of traces, we found that increasing $[K^+]_o$ affected the balance between slow- and fast-kinetic components, favouring the latter. The results yielded saturable curves with respect to K^+ concentration that fitted well to the Hill equation [25]:

$$f_a = f_o + f_{max} \cdot [K^+]^h / \left(K_{1/2}{}^h + [K^+]^h\right) \quad (2)$$

where h is the Hill (co-operativity) coefficient and $K_{1/2}$ is the apparent half-saturation constant for the K^+-dependence of the fractional amplitude. Both independent and joint fittings with h held in common between the mutants gave similar results. The joint fitting shown in Figure 3(A) yielded a Hill coefficient of 2.1 ± 0.4, consistent with the co-operative binding of two K^+ ions and in agreement with previous results [19,21].

A comparison of the Leu^{270} mutants with wild-type TOK1 characteristics showed a lower apparent affinity for K^+ associated with all of the mutants, although the effect for L270D was not very significant (Figure 3B). L270W and L270Y exhibited apparent affinities for K^+ reduced approx. 30- and 40-fold, while the affinity for K^+ was less affected for L270A and L270F. An analysis of $K_{1/2}$ values with the residue charge, van der Waals volumes (V) and accessible surface areas (A) of these mutants (Figure 3B, lower panel) suggested that spatial packing, rather than residue polarity or hydrophilicity, was a key determinant of the mutational effects, with the apparent $K_{1/2}$ rising from a minimum value as V and A deviated either side of values near 120 Å^3 (1 Å = 0.1 nm) and 180 Å^2 respectively. Additional replacement with lysine supported this interpretation, giving currents that were indistinguishable from wild-type TOK1 (see the Supplementary Table at http://www.BiochemJ.org/bj/393/bj3930645add.htm).

Figure 3(A) also shows a reduction in the minimum fractional amplitude, f_a, which approached zero for all of the mutants, albeit to a lesser extent for L270D. This characteristic is immediately evident in the current traces in Figure 2, which show currents evoked by L270D were similar to the wild-type currents in 10 and 3 mM K^+ but, at lower $[K^+]$, were dominated by the slow component when compared with the wild-type current. Thus mutations of Leu^{270} appeared to affect the dynamic range for f_a. A straightforward interpretation of this effect is that, when closed, the mutations favoured conformations of TOK1 in more distal closed states of the channel. We return to this point below (see the Discussion).

Mutations at Leu^{270} affect the K^+-sensitivity of deactivation

The extremely fast (1–2 ms) deactivation kinetics of TOK1 preclude its analysis using tail currents. Instead, we used a two-pulse protocol with varying interpulse intervals to assess the time course

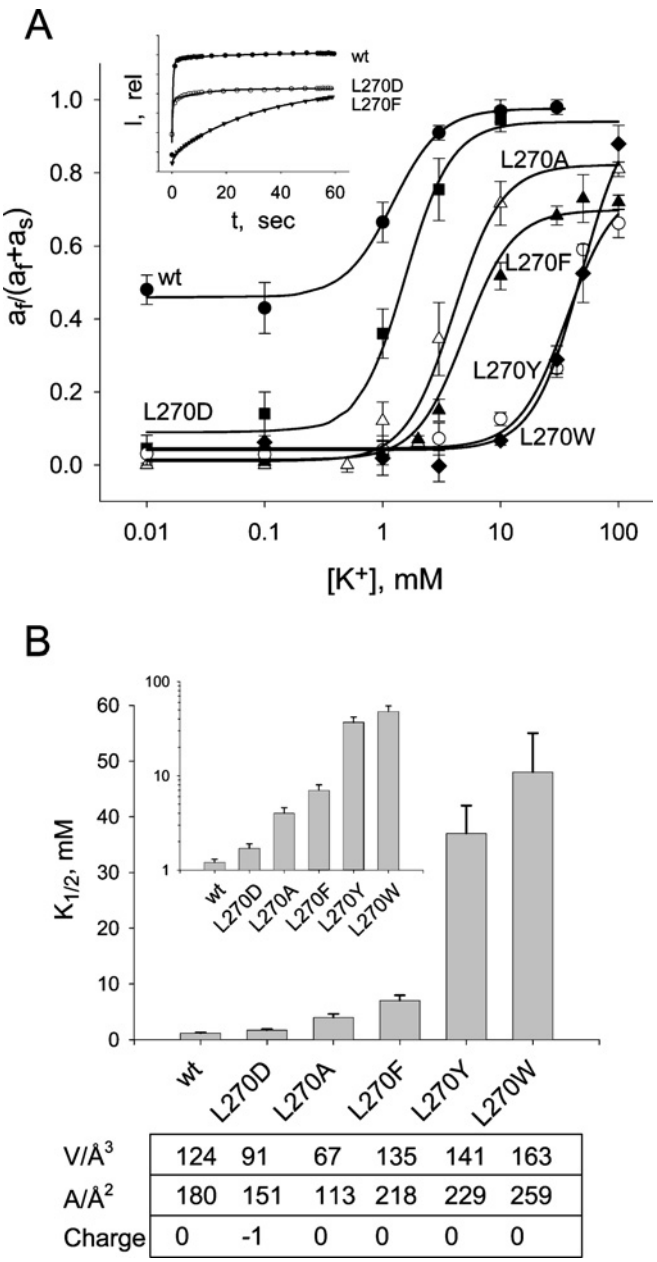

	wt	L270D	L270A	L270F	L270Y	L270W
V/Å^3	124	91	67	135	141	163
A/Å^2	180	151	113	218	229	259
Charge	0	-1	0	0	0	0

Figure 3 Mutations of Leu^{270} decrease the affinity for external K^+ in TOK1 activation

(**A**) The amplitude of the fast component of the current as a fraction of the total amplitudes of the time-dependent components plotted against $[K^+]_o$. Results are means ± S.E.M. for four to five oocytes. Amplitudes were derived from fittings to eqn 1 with k_f and k_s held in common for each mutant. Solid lines represent joint fittings to the Hill equation (eqn 2) with the Hill coefficient, h, held in common. Fitted parameters:

	wt ●	L270D ■	L270A △	L270F ▲	L270Y ○	L270W ◆
y_0	0.46 ± 0.04	0.10 ± 0.04	0.01 ± 0.03	0.01 ± 0.04	0.05 ± 0.03	0.04 ± 0.03
y_{max}	0.52 ± 0.06	0.84 ± 0.07	0.81 ± 0.1	0.68 ± 0.05	0.72 ± 0.1	0.96 ± 0.1
$K_{1/2}$(mM)	1.1 ± 0.3	1.7 ± 0.2	4.0 ± 0.9	6.0 ± 0.8	37 ± 7	48 ± 9

$h = 2.1 \pm 0.4$. The inset shows an example of fittings (solid lines) of current trajectories in 3 mM K^+ to sums of exponentials for wild-type (wt), L270D and L270F. (**B**) $K_{1/2}$ values derived from the fittings in (**A**) for wild-type and the mutants. The inset shows $K_{1/2}$ values plotted on logarithmic scale. The van der Waals volume (V), the accessible surface area (A) and the charge at pH 7 of the residues replacing leucine shown in the Table are taken from [50].

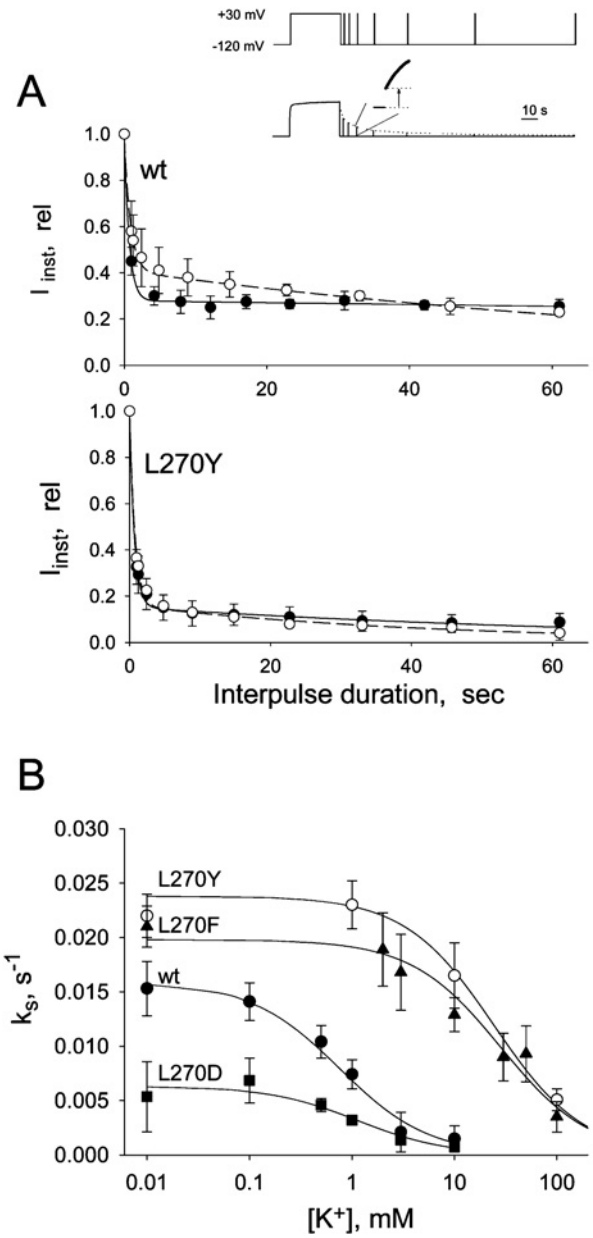

Figure 4 Mutations of Leu^{270} affect the affinity for K$^+$ in TOK1 deactivation

(**A**) Escape from the instantaneously activating state. Fractions of steady-state current determined on steps to +30 mV after time intervals at −120 mV as indicated. Representative data for wild-type TOK1 and L270Y mutant currents fitted to sums of two exponentials: broken lines, 1 mM K^+; solid lines, 10 mM K^+. The inset shows a schematic diagram of pulse cycle protocol. See text for details. (**B**) Rate constant of the slow component as a function of $[K^+]_o$ for wild-type (wt, ●), L270D (■), L270F (▲) and L270Y (○). Results are means ± S.E.M. for three to five oocytes. Curves are fittings to a logistic function (eqn 4). Fitted parameters: $R = 0.016 \pm 0.002$ (wild-type), 0.0063 ± 0.0008 (L270D), 0.020 ± 0.003 (L270F) and 0.024 ± 0.0008; $K_{1/2} = 0.8 \pm 0.3$ (wild-type), 1.5 ± 0.3 (L270D), 24 ± 14 (L270F) and 28 ± 4 (L270Y) mM.

for escape from the proximal closed state of the channel to more distal closed states. TOK1 current was activated by stepping the voltage to +30 mV for 30 s, followed by a step to −120 mV for periods of 1–61 s. The channel population remaining in the instantaneously activatable pool at the end of this period was then determined by measuring the current on a second step to +30 mV (see Figure 4A, inset).

Figure 4(A) shows the results of two such experiments with wild-type TOK1 and the mutant L270Y. For comparison, the instantaneous current amplitude was determined and normalized to the steady-state current recorded at the end of the first +30 mV step before plotting as a function of interpulse duration. The resulting escape kinetics exhibited two components, as reported previously [19], and were well-fitted as shown to a sum of exponentials of the form

$$I_{inst} = d_f e^{-k_f t} + d_s e^{-k_s t} \quad (3)$$

where d_f and d_s are the relative amplitudes of the fast and slow components respectively, and k_f and k_s are the corresponding rate constants. From a comparison of relaxations (Figure 4A), it is evident that the L270Y mutant strongly affected the slow-relaxing component of this current at both 1 and 10 mM K^+. We analysed the deactivation characteristics for the wild-type and each of the Leu^{270} mutants in this manner to derive the rate constants as a function of K^+ concentration. As reported previously [19,21], only the rate constant for the slow-relaxing component, k_s, showed an appreciable dependence on $[K^+]_o$ and was subject to mutations affecting the K^+-sensitivity of TOK1. Mean values of k_s for selected Leu^{270} mutations are plotted in Figure 4(B), fitted to a logistic function

$$k_s = R\{1 + ([K^+]/K_{1/2})\} \quad (4)$$

where the apparent $K_{1/2}$ corresponds to the $[K^+]$ at which k_s gives the half-maximum value of the response amplitude R. This analysis yielded a $K_{1/2}$ for the wild-type channel of 0.8 mM, consistent with Vergani et al. [19] and a similar value for the L270D mutant (see Figure 4B). Again, $K_{1/2}$ values for L270F and L270Y mutants were displaced to higher K^+ concentrations, indicating approx. 30- and 35-fold decreases in apparent affinity. Results for L270W and L270A gave $K_{1/2}$ values of 37 ± 3 and 7 ± 2 mM respectively (results not shown). Thus, in each case, k_s increased at any one $[K^+]_o$, consistent with a preferred residence in more distal closed states at low $[K^+]_o$ and in agreement with the channel activation behaviour; with the exception of L270D, for the Leu^{270} mutants the effect of amino acid substitutions was to accelerate transfer into these distal closed states and to reduce the sensitivity of this process to extracellular K^+. For L270D, the effect of substitution was an overall reduction in the efficacy of $[K^+]_o$ (i.e. on the dynamic range for k_s) without a significant effect on $K_{1/2}$. In short, mutations of Leu^{270} affected the channel behaviour in response to K^+ not only during activation, but also during deactivation, with an overall trend to a reduced affinity for $[K^+]_o$.

Leu^{270} mutants invert the K$^+$-sensitivity of TOK1 conductance

External K^+ concentrations near and above 10 mM normally suppresses channel gating, resulting in a positive shift in the steady-state IV relationship as $[K^+]_o$ increases (see the Introduction). Figure 5 shows that a similar behaviour, if somewhat reduced, was observed for the L270D mutant. However, the same was not true for the L270F and L270Y mutants. Currents for these Leu^{270} substitutions gave steady-state characteristics with 10, 30 and 100 mM $[K^+]_o$ that were visibly different in their voltage-dependence from the wild-type current. To analyse the currents, relative conductances (Figure 5, insets) were determined from joint fittings of the IV curves for each construct to a modified Boltzmann function [19]:

$$I = [G_{max}(V - E_K)]/\left(1 + e^{dF(V - V_{1/2})/RT}\right) \quad (5)$$

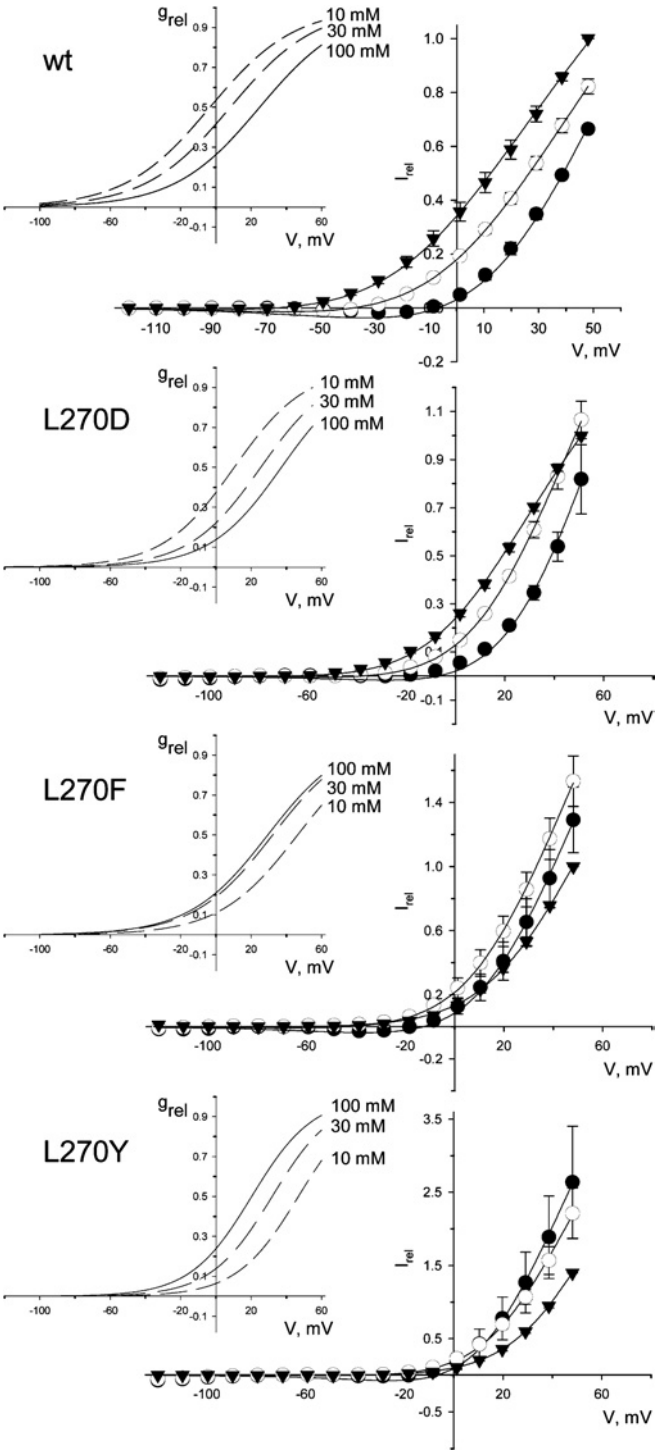

Figure 5 Leu^{270} mutations affect voltage-dependent (low-affinity) K$^+$ dependence of TOK1

Current–voltage (IV) relationships for wild-type (wt), L270D, L270F and L270Y measured in 10 (▼), 30 (○) or 100 (●) mM K^+. Steady-state currents were measured by stepping the voltage from a holding potential of −120 mV to increasingly positive voltages of between −120 and +50 mV at 10 mV intervals for 10 s before returning to the holding potential, and the current at the end of the pulse was measured (wild-type and L270D). For L270F and L270Y, test pulses were extended to 30 s in order to approach steady-state. Results are means ± S.E.M. for four to five oocytes. Currents between different batches of oocytes were normalized to internal standards (current at 50 mV in 10 mM K^+) for each construct. Solid lines represent joint fittings to the Boltzmann equation (eqn 5) with the voltage sensitivity coefficient (d) and internal $[K^+]$ ($[K^+]_i$) held in common.

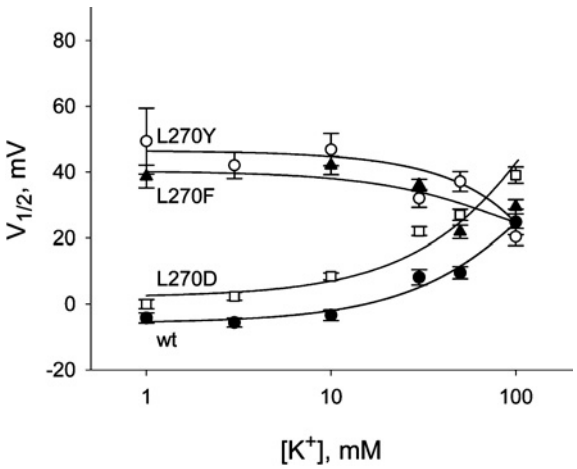

Figure 6 $V_{1/2}$ values for gating of wild-type and L270Y and L270F mutants of TOK1

$V_{1/2}$ values were calculated as described in Figure 5 for wild-type (wt, ●, five cells), L270D (□, four cells), L270F (▲, four cells) and L270Y (○, five cells). The data were fitted empirically to second-order polynomial functions for visual clarity.

where I is the current at voltage V, G_{max} is the maximum steady-state conductance, d is the voltage sensitivity coefficient, $V_{1/2}$ is the voltage giving half-maximal steady-state conductance, and F, R and T have their usual meanings.

The analysis yielded voltage-sensitivity coefficients for the mutants that did not differ significantly from the wild-type or change with variation in $[K^+]_o$, and a close inspection of the GV curves shows a general reduction in relative conductance near and negative from 0 mV in all three mutants. However, the most striking feature of these data and the derived GV curves is the virtual absence from the L270F and L270Y mutants of a positive shift in the IV curve when $[K^+]_o$ was increased from 10 to 30 or 100 mM K^+. Indeed, for both of these mutants, increasing $[K^+]_o$ promoted the current at voltages near and positive from 0 mV, indicating an increase in conductance and negative shift in the GV curve (Figure 5, insets) with increasing $[K^+]_o$. These results are summarized in Figure 6. Plotting as a function of $[K^+]_o$ here shows an overall positive displacement of $V_{1/2}$ in each of the mutants, notably at $[K^+]_o$ values of 10 mM and below. Figure 6 also shows that $V_{1/2}$ was shifted positive with increasing $[K^+]_o$ in wild-type TOK1 and the L270D mutant, but, for the L270F and L270Y mutants, increasing $[K^+]_o$ above 10 mM led to a negative

	wt	L270D	L270F	L270Y
$[K^+]_i$ (mM)	132 ± 6	130 ± 8	148 ± 7	129 ± 8
d	1.04 ± 0.04	1.23 ± 0.03	1.13 ± 0.04	1.31 ± 0.07
G_{max} (10 mM K^+)	0.0097 ± 0.0002	0.0097 ± 0.0002	0.015 ± 0.001	0.018 ± 0.003
G_{max} (30 mM K^+)	0.011 ± 0.0003	0.015 ± 0.0004	0.024 ± 0.0008	0.030 ± 0.002
G_{max} (100 mM K^+)	0.017 ± 0.001	0.021 ± 0.0009	0.029 ± 0.001	0.047 ± 0.002
$V_{1/2}$ (10 mM K^+) (mV)	−3.4 ± 2	10.4 ± 1	46 ± 3	55 ± 5
$V_{1/2}$ (30 mM K^+) (mV)	8.1 ± 2	25 ± 1	32 ± 2	38 ± 3
$V_{1/2}$ (100 mM K^+) (mV)	25 ± 4	37 ± 3	29 ± 2	26 ± 2

Insets show the relative conductance G_{rel} (= G/G_{max}) as a function of voltage, calculated from the fitted parameters of the corresponding IV curves. Best fittings (as shown) were obtained holding d and E_K in common and allowing only G_{max} and $V_{1/2}$ to vary between data sets. Similar results were obtained for steady-state currents estimated by extrapolating fitted current trajectories as in Figure 3(A), inset, to eqn 1.

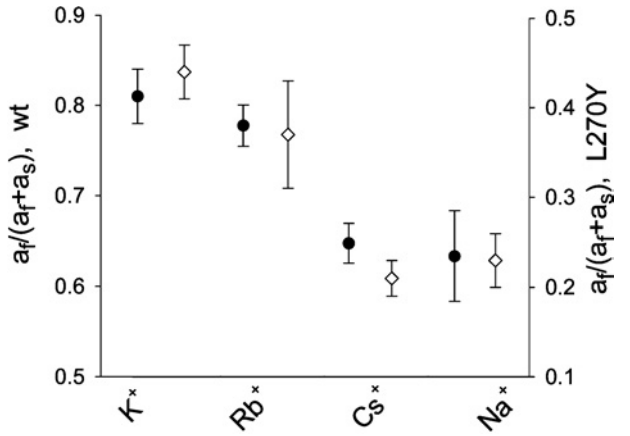

Figure 7 Ion selectivities for TOK1 activation kinetics in wild-type and the L270Y mutant

K^+ and Rb^+ are more efficient than Cs^+ and Na^+ in accelerating activation kinetics for both the wild-type (wt, ●) and L270Y (◇). The amplitude of the fast component of the current is given as a fraction of the total amplitudes of the time-dependent components derived from fittings to eqn 1 as in Figure 3. Bath solutions contained 30 mM KCl, RbCl, CsCl or NaCl as labelled. Results are means ± S.E.M. for three to five oocytes.

Table 1 Ionic selectivity for gating, determined as $V_{1/2}$ of steady-state currents for wild-type TOK1 and the L270Y mutant

$V_{1/2}$ was determined in 10 mM of each cation from joint fitting to eqn 5. Data are from three to four experiments in each case.

	$V_{1/2}$ (mV) ... K^+	Rb^+	Cs^+	Na^+
Wild-type	+3 ± 2	+12 ± 1	+9 ± 2	−34 ± 5
L270Y	+10 ± 2	+23 ± 3	+34 ± 4	−32 ± 3

shift in $V_{1/2}$. In other words, these mutations of Leu^{270} actually effected a reversal in the response to K^+ in the low-affinity range, so that increasing $[K^+]_o$ favours the open state of the channel.

Cation selectivities differ between gating and permeation

An important question is whether these mutations are associated directly with K^+ binding at the extracellular surface of the channel, or whether their effects might be mediated indirectly through long-distance conformational changes of the protein, for example to binding sites within the permeation pathway. Mutations affecting cation binding at sites removed from the pore might be expected to leave ion selectivity for permeation unaffected, whereas, if cation binding for permeation and gating overlapped, it would follow that both processes should be affected. To address this question, we examined the effect of other univalent cations, first on the fractional amplitude distribution, f_a, and secondly on $V_{1/2}$ values for steady-state conductance with the wild-type TOK1 and L270Y mutant, and we compared these results with the effects of mutation on the selectivity for permeation.

Fractional amplitudes and values for $V_{1/2}$ were determined as above (see Figures 3 and 5), replacing extracellular K^+ with equivalent concentrations of Cs^+, Rb^+ and Na^+. As summarized in Figure 7 and Table 1, these analyses yielded different results for the two gating responses. Steady-state conductances determined in 10 and 30 mM concentrations of the alkali cations gave values for $V_{1/2}$ in the sequence $Rb^+ > Cs^+ > K^+ > Na^+$ (Eisenman Series II) for the wild-type TOK1 current and $Cs^+ > Rb^+ > K^+ > Na^+$ (Eisenman Series I) for the L270Y mutant, consistent with previous results and the effects of the more extreme A428Y mutation [19,21,26], and indicating a decrease in apparent field strength [1]. In contrast, we found the fractional amplitude to be unaffected by the L270Y mutation: in each case, f_a yielded the sequence $K^+ > Rb^+ > Cs^+ > Na^+$ (Eisenman Series IV) for efficacy in promoting the fast-activating current kinetics, although the activation kinetics were generally slower in the mutant (Figure 7). Again, equivalent results were obtained previously for the wild-type TOK1 and A428Y mutant line [19], and the comparison with the $V_{1/2}$ results thus supports the view of two kinetically distinct processes with different binding affinities and mutational sensitivities.

Table 2 Relative ionic selectivity for permeation of wild-type TOK1 and the L270Y mutant

Relative permeabilities, P_X/P_K, were determined under bi-ionic conditions using the Constant Field assumption. Current reversal voltages were estimated by chord conductance extrapolations from instantaneous currents recorded at voltages between 0 and +60 mV. Data are from three experiments in each case.

	Cs^+	Rb^+	Na^+
Wild-type	0.89 ± 0.02	0.84 ± 0.03	< 0.03
L270Y	0.88 ± 0.03	0.83 ± 0.04	< 0.03

To determine the selectivity for permeation, a two-step protocol was employed starting from holding voltages between −120 and 0 mV, and stepping to voltages between 0 and +60 mV. Again, because the extremely fast deactivation kinetics of TOK1 precluded measurements of tail currents, and hence of the tail current reversal voltage (E_{rev}) directly, we estimated values of E_{rev} for each of the alkali cations by extrapolating chord conductances to a common point of intersection (cf. Figure 2 in [18]). Measurements were carried out under bi-ionic conditions with substitutions at 30 mM concentrations to minimize errors that might be introduced by intrinsic rectification of the current. These results are summarized in Table 2 and show that, both for wild-type TOK1 and L270Y currents, substituting Rb^+ and Cs^+ were only marginally less effective in gaining access to the channel pore than K^+, whereas substituting Na^+ gave E_{rev} values displaced substantially to negative voltages. The wild-type and L270Y data showed no significant difference for any of the substitutions, giving the same selectivity sequence $K^+ > Cs^+ \geqslant Rb^+ \gg Na^+$ (Eisenman Series IV). Thus the L270Y mutation does not appear to affect properties of the pore in its binding of the cations. A comparison with the corresponding data for wild-type TOK1 and L270Y gating (Figure 7 and Table 1) indicates differences in selectivity among the cations for the high-affinity response (f_a), and a qualitative difference in selectivity and sensitivity to the L270Y mutation for the low-affinity response ($V_{1/2}$ and steady-state conductance).

It should be noted that the ion selectivity for permeation as we describe it is derived from equilibrium characteristics, whereas selectivities for gating are necessarily determined at voltages away from equilibrium. In principle, the relative ability of ions to bind within the selectivity filter of a channel at equilibrium may differ from their ability to permeate the channel, and hence carry current, which reflects ion binding as well as release and passage through the pore [1]. However, since the question of selectivity for alkali cation sensing, in the first instance, is a question of the relative abilities for binding of the different cations in the selectivity filter, the comparison is arguably the most appropriate. Thus a simple explanation for the differences in selectivity between gating and permeation, and furthermore the relative effects of mutation, is that they reflect distinct physical properties of the binding sites for gating and for permeation.

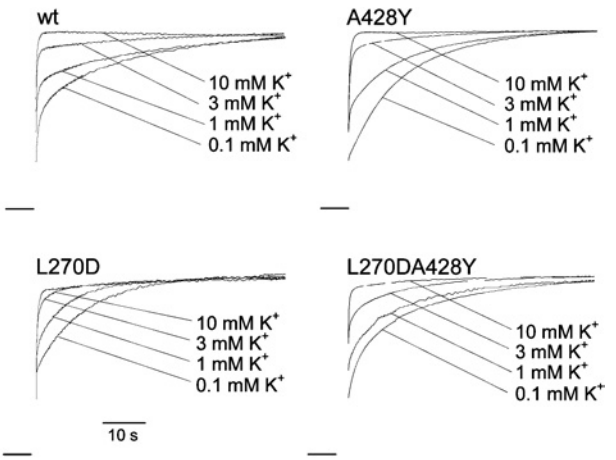

Figure 8 Mutant interaction between pore domains in TOK1 activation

The double mutant L270D/A428Y slows activation of TOK1 in low $[K^+]$. Current trajectories for wild-type (wt), L270D, A428Y and L270D/A428Y in 0.1, 1, 3 or 10 mM K^+ are indicated. The membrane voltage was stepped from a holding potential of − 120 mV to + 30 mV for 60 s before returning to − 120 mV. Current traces are normalized to the estimated current maximum. The zero current level is indicated to the left of each set of traces. Scale bar, 10 s.

Leu^{270} and Ala^{428} mutants interact

Previous results had indicated that the two pore loops are able to function semi-autonomously [20] and that effects of mutations in the two pore domains are not interactive [19,21]. We were therefore intrigued by the dramatic effects of amino acid substitutions at position Leu^{270} and our failure to recover functional mutants when targeting the corresponding position in P2 (see above). To explore these relationships further, we constructed double mutants by combining mutants of Leu^{270} with the P2 mutant A428Y characterized previously by Vergani et al. [19] to test for pore domain interactions. The latter residue is situated just C-terminal of the GYGD selectivity filter in the pore loop (Figure 1) and its mutation, like that of Leu^{270}, affects both high- and low-affinity K^+-dependent gating responses. Vergani et al. [19] found Ala^{428} substitutions led to slow activation kinetics at low $[K^+]$ (see Figure 8) and a decreased sensitivity to K^+ both in the fractional amplitude and deactivation kinetics, and in the voltage displacement of the steady-state conductance.

Of the double mutants constructed, L270Y/A428Y failed to give measurable currents under any voltage-clamp regime (see the Supplementary Table at http://www.BiochemJ.org/bj/393/bj3930645add.htm). The double mutant L270D/A428Y, on the other hand, yielded currents on positive voltage steps that showed activation kinetics at low $[K^+]$ more closely allied to that of A428Y than of L270D, albeit with a reduced slow-kinetic component (Figure 8). We calculated the fractional amplitudes, f_a, for each of the constructs as before, plotting the results as a function of $[K^+]_o$. As before, joint fitting to the Hill equation (eqn 2) yielded visually satisfactory and statistically best results with the K^+-dependence and a coefficient of approx. 2 for all four data sets (Figure 9A). We found that the apparent affinity for K^+ was decreased in the mutant L270D/A428Y as compared with the wild type, but increased somewhat relative to that of the A428Y mutant (Figure 9, legend). A stronger interaction between the two sites was evident when the dynamic range and minimum values for f_a were taken into account (Figure 9A). For the wild-type TOK1, the fractional current approached a minimum near 0.4 at $[K^+]_o$ below 1 mM, and for the L270D and A428Y mutants, f_a approached values of 0 and − 0.3 respectively (in the latter case,

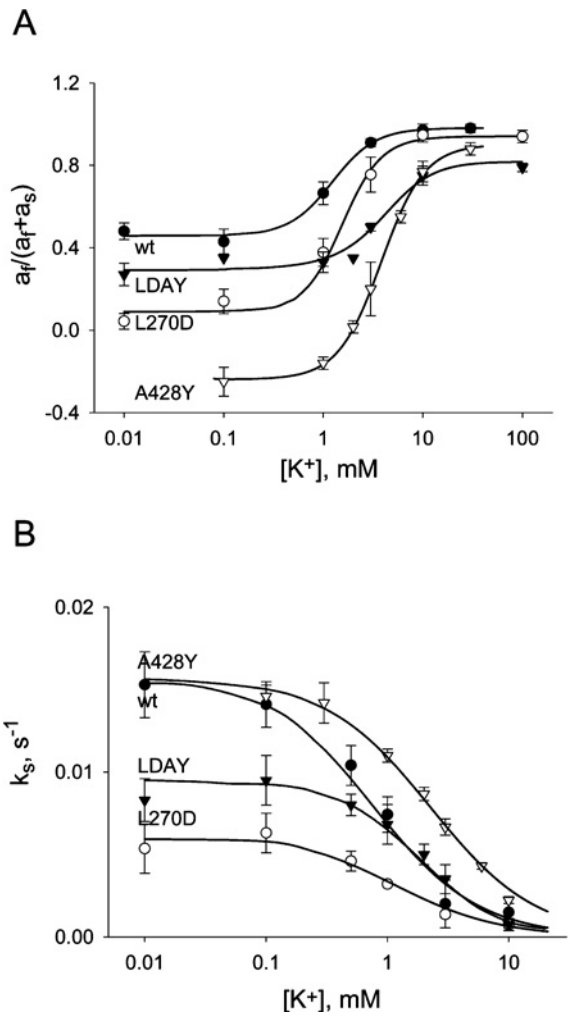

Figure 9 Analysis of mutant interaction between pore domains in TOK1

L270D/A428Y compensates for the effect of the single mutants both during activation and deactivation. (**A**) The amplitude of the fast component of the current as a fraction of the total amplitudes of the time-dependent components plotted against $[K^+]_o$ for wild-type (wt, ●), L270D (○), A428Y (▽) and L270D/A428Y (▼). Results are means ± S.E.M. for three to five oocytes. Solid lines represent joint fittings to the Hill equation (eqn 2) with the Hill coefficient, h, held in common. Fitted parameters:

	wt	L270D	A428Y	L270D/A428Y
y_0	0.46 ± 0.04	0.10 ± 0.04	− 0.24 ± 0.02	0.34 ± 0.03
y_{max}	0.52 ± 0.06	0.85 ± 0.09	1.14 ± 0.08	0.54 ± 0.08
$K_{1/2}$ (mM)	1.1 ± 0.3	1.7 ± 0.2	3.9 ± 0.3	2.7 ± 0.4

$h = 2.0 \pm 0.4$. (**B**) Rate constant of the slow component as a function of $[K^+]_o$. Results are means ± S.E.M. for three to five oocytes. Curves are fittings to a logistic function (eqn 4). Fitted parameters: R = 0.016 ± 0.002 (wild-type), 0.0063 ± 0.0008 (L270D), 0.016 ± 0.002 (A428Y) and 0.0096 ± 0.001 (L270D/A428Y), $K_{1/2} = 0.8 \pm 0.3$ (wild-type), 1.1 ± 0.4 (L270D), 2.3 ± 0.3 (A428Y) and 1.3 ± 0.2 (L270D/A428Y) mM.

reflecting a sigmoidicity to the current trajectories in low $[K^+]_o$; see also Vergani et al. [19]). For the L270D/A428Y mutant, however, we found the minimum fractional amplitude situated near a value of 0.3, significantly greater than for either of the single mutants and close to that of the wild-type current.

Inspection of the deactivation kinetics for the L270D/A428Y mutant also yielded evidence of interaction between the two pore domains. Figure 9(B) summarizes analyses of the rate of

escape from the instantaneously activatable pool (see Figure 4). Again, relaxations (results not shown) were well-fitted to eqn 3 and gave rate constants for the slow-kinetic component that declined as a function of $[K^+]_o$. In this case, the L270D/A428Y mutant yielded an apparent affinity for K^+ similar to the L270D mutant, but a maximum rate ($t_{1/2}$ minimum) of the slow-kinetic component at low $[K^+]_o$ that was distinct from that of either single mutant. In other words, characteristics of the L270D/A428Y mutant deactivation neither reflected the single mutants nor a sum of these [27], but, instead, suggest an unexpected degree of interaction between the pore loops and co-operativity in gating. We return to these findings below.

DISCUSSION

The *S. cerevisiae* K^+ channel TOK1 is gated by external K^+, a feature intrinsic to the channel protein. Previous studies of the mechanism of regulation by K^+ in TOK1 yielded clues to roles for internal domains of the channel that contribute to gating [22,28] and to external domains that are important for the external K^+-sensitivity of gating [19,21]. These latter studies identified distinct effects of external K^+ with different kinetic dependencies, leading to the hypothesis that K^+ binds at two discrete sites on the channel protein. Because both putative K^+-binding sites appeared to be associated with each of the two TOK1 pore domains, and because mutations at selected residues failed to show a synergy in gating modification [21], they also provided *de facto* support for the argument that the two pore domains of TOK1 function semi-autonomously [20]. In the present paper, we report the identification of a single residue position, associated with Leu^{270} in the first pore domain of TOK1, of critical importance to the K^+-dependence for gating, and we demonstrate an underlying, but subtle, interaction between pore domains of this unusual K^+ channel. Key observations are: (i) TOK1 gating and its K^+-dependence were found to be acutely sensitive to substitutions that affect residue packing in the first (P1) pore domain at position Leu^{270}, while all substitutions at the corresponding site in the second (P2) pore domain failed to give functional channels; (ii) Leu^{270} substitutions affected the kinetic characteristics of gating associated with both putative K^+-binding sites, in the most extreme cases actually inverting the K^+-sensitivity of the steady-state conductance for TOK1; (iii) Leu^{270} substitution altered the apparent alkali cation selectivities for gating, but not the selectivity for permeation; and (iv) the relatively mild mutation L270D partially rescued wild-type TOK1 characteristics in the double mutant L270D/A428Y. These and additional data lend support to the idea that gating is regulated by K^+ binding in external pockets that are distinct from the selectivity filter in the permeation pathway. They also offer primary evidence for a gating interaction between pore domains that is reflected in the K^+-sensitivity of this unusual K^+ channel.

Mapping TOK1 pore domains to target key residues of putative K^+-binding pockets

Our strategy in selecting candidates for site-directed mutagenesis was to map the pore domains of TOK1 to the crystal structures of the bacterial KcsA [8], MthK [23], KvAP [6] and Kv1.2 K^+ channels [5]. The crystal structures of KcsA and KvAP are believed to be of the closed channels, whereas MthK was crystallized in the open conformation in the presence of Ca^{2+}. The structures differ mainly in those parts of the channels that are to the cytosolic side of the membrane from the selectivity filter and associated with the internal S6 gate. TOK1 maps satisfactorily to the KcsA structure [19] and to that of the KvAP and Kv1.2 K^+ channels using SWISS-MODEL (http://www.expasy.org/spdbv/) [29–31]. However, it gave a marginally closer fit to the MthK K^+ channel pore domain (PDB code 1LNQ; http://srs.ebi.ac.uk) – for P1, residues Ser^{247}–Arg^{323} and, for P2, residues Ser^{381}–Val^{457} – to the MthK sequence between residues Pro^{19} and Leu^{98} that spans the pore loop and helix and the two adjacent membrane-spanning domains. This analysis uncovered two short segments, one in each pore domain, that appeared to juxtapose with residues shown previously to affect the K^+-sensitivity of TOK1 gating [19,21].

Figure 1(B) shows results for the first pore domain (P1) of TOK1 with the key residues Leu^{270}, Asn^{276} and Leu^{293} highlighted in space-filling display. Similar analysis of the P2 domain identified Glu^{404} in juxtaposition with both Asn^{410} and Ala^{428}. The adjacent residues, His^{271} in P1, Ala^{403} and Asn^{405} in P2, were also identified as secondary targets for study (see also Figure 1A). In fact, residue positions 270 (P1) and 404 (P2) proved to be exquisitely sensitive to substitution, the latter failing to yield measurable currents even with the most conservative amino acid replacements. Furthermore, conservative mutations of Leu^{270} (P1), for example with alanine, resulted in visible changes in gating kinetics, and larger side-chain substitutions resulted in current gating with characteristics consistent with more than a 30-fold decrease in apparent affinity for K^+ (Figures 2–4) and inversion of the K^+-dependence of the steady-state conductance (Figures 5 and 6). In contrast, residue substitutions at the other three positions generally yielded TOK1 current with wild-type characteristics, with the exceptions of A403D and A403K that failed to give measurable currents. Thus mutation and electrophysiological analysis support the basic predictions of the structural modelling.

Locating K^+-binding sites for TOK1 gating

In itself, mapping TOK1 to crystallographic structures of the bacterial K^+ channels is useful primarily as a predictive tool for mutagenic studies and their interpretation, rather than a means of identifying any K^+-binding sites. Nonetheless, several lines of evidence now support the idea of two closely associated binding sites for K^+ for which Leu^{270} provides a landmark. (i) Characteristics of the Leu^{270} mutants clearly show that substitution of this residue alters TOK1 gating in two distinct kinetic characteristics; (ii) analysis of the structural correlates for each of the Leu^{270} substitutions (see Figures 3 and 5) confirm the importance of residue packing within the protein, rather than side-group charge or polarity, in the K^+-sensitivity for gating and, indeed, reveal comparable effects on gating even with mutations such as L270D and L270A that reduced the van der Waals volume and exposed surface area of the residue; (iii) selectivities among alkali cations indicated that binding in the G(Y/L)GD selectivity filter during permeation of TOK1 is characterized by the sequence $K^+ > Cs^+ \geqslant Rb^+ > Na^+$ (Table 1), whereas gating was associated with the sequences $K^+ > Rb^+ > Cs^+ > Na^+$ for the high-affinity (fractional amplitude) and $Rb^+ > Cs^+ > K^+ > Na^+$ for the low-affinity (steady-state conductance) responses (Figure 7 and Table 1); (iv) finally, the L270Y mutation, like A428Y [19], had no qualitative effect on selectivity either for binding within the pore or for the high-affinity response in gating, but it affected cation selectivity for low-affinity response in gating consistent with a decrease in field strength at the K^+-binding site. The latter two observations parallel those of Vergani et al. [19] who reached much the same conclusion for residues Leu^{293} and Ala^{428} positioned just C-terminal to each of the pore loops. Indeed, the strong effect of substitutions at position 270 suggests a close association to sites that are critical for K^+ binding. The importance of residue size, with effects either side of an optimum

exposed surface area near 180 Å, indicates that conformation of the protein backbone and, furthermore, its spatial positioning, not simply its packing, is critical to the K^+-sensitivity of gating. Finally, the differences in cation selectivity and their sensitivity to Leu^{270} substitutions, point to different physical properties for cation binding in gating and in permeation

One interpretation for TOK1 gating has posited a dual role for the pore loop of the channel in determining both the ion selectivity in permeation and the sensitivity of the gating mechanism to K^+ [22,28]. Formally, this idea is equivalent to 'foot-in-the-door' gating, analogous to C-type inactivation of many Kv channels [32–34], in which cation occupation of the selectivity filter within the pore suppresses closure of an internal gate and access to the pore from inside through allosteric conformational changes in channel structure. An attraction of this model is its 'economy of structure', incorporating analogous functions of ion selectivity and cation sensing for gating within a single binding domain. Its difficulties rest with the underlying assumption *ad hoc* that binding within the filter has entirely opposing actions on gating on K^+ access from inside [28]. It also implies that ion selectivity for gating and for permeation (or, at least, for binding within the selectivity filter) are identical, a prediction that is not supported by our results (Figure 7 and Tables 1 and 2).

We favour the alternative, and structurally non-minimalist, interpretation of physically distinct binding sites for K^+ (and other alkali cations) with different effects on permeation and on gating. This postulate accords with our evidence for a ring-like cluster of residues associated with each pore domain on the outer surface of the TOK1 protein that strongly affect the K^+-dependence of gating and could provide oxygens for co-ordinating alkali cations (see Figure 1). Consequently, it accommodates differences in cation selectivities between permeation and gating that, based on the results above, imply at least three K^+-co-ordination sites, two associated with gating and its sensitivity to K^+ outside, and a third with permeation. It is of interest that this interpretation for the K^+-sensitivity of TOK1 finds parallels with that of the K^+-enhanced activity of the weakly rectifying K^+ channel AKT3 of *Arabidopsis*. For AKT3, like TOK1, substitutions of residues positioned either side of the pore loop strongly influence acid- and K^+-mediated activation of the current [35]. Several voltage-gated K^+ channels in animal cells also exhibit sensitivities to extracellular K^+ [36], including the inward-rectifying ROMK (renal outer medullary K^+) channel [37] for which a site of action has been suggested to lie near the outer mouth of the pore [38–40]. However, in all of these cases, the voltage-dependence for gating itself is unaffected by K^+.

Only in the plant SKOR (stelar K^+ outward rectifying) and GORK (guard cell outward rectifying K^+) channels does the voltage-dependence of gating shift in parallel with E_K in a manner similar to TOK1 [41,42]. Intriguingly, the K^+-sensitivity of these K^+ channels appears to proceed via a different mechanism, although the overall effect on current kinetics and steady-state conductance are very similar [43–46]. A recent study of the *Arabidopsis* SKOR channel [47] failed to identify any effect of substitutions within domains of the channel exposed to the extracellular surface of the membrane, including residue paralogues to those associated with the K^+-sensitivity of TOK1. Thus it appears that evolution has solved the problem of K^+-dependent gating in at least two different ways at the molecular level.

K^+-sensitivity of TOK1 gating uncovers K^+ channel pore domain interactions

These studies now also offer direct evidence for a synergy between pore domains that affects gating directly through its apparent K^+ affinity. The effects differ fundamentally from cross-domain interactions associated with permeation that are evident when the TOK1 pore domains are expressed individually [20]. We found that kinetic characteristics of the single mutants L270D in P1 and A428Y in P2 compensate for one another in the double mutant L270D/A428Y, leading to a partial restoration of wild-type TOK1 gating (Figures 8 and 9). Intriguingly, a similar approach in one previous study failed to identify such cross-domain interactions: Vergani and Blatt [21] reported that the double mutant N276D/N410D yielded activation and deactivation kinetics equivalent to the sum of the characteristics for the individual mutants, N276D in P1 and N410D in P2. One important difference is that Asn^{276} and Asn^{410} reside at equivalent positions, both in the extracellular loops N-terminal of the two pore helices (see Figure 1). These mutants also differ in that they affected TOK1 K^+-sensitivity that is associated with the high-affinity response, but showed no influence on the K^+-dependence of the steady-state conductance (compare with Figure 5). Furthermore, N276D and N410D highlighted qualitative differences between the two pore domains: the effects of the substitutions were most apparent in the activation kinetics for N410D and in deactivation kinetics for N276D. In contrast, Leu^{270} and Ala^{428} are situated cross-positionally on extracellular loops within the two domains, Leu^{270} in the N-terminal loop of P1 and Ala^{428} in the C-terminal loop of P2; substitutions at these two sites influence TOK1 gating both in the high-affinity and in the low-affinity K^+-dependencies; finally, the effects of substitutions at Leu^{270} and Ala^{428} are qualitatively similar (compare with Vergani et al. [19]). Clearly these differences are structurally correlated, although the most important physical characteristics remain to be determined.

It is of interest that interactions between subunits are also characteristic of voltage-dependent gating in K^+ channels of the Kv family [9,10,48] and the parallel raises a question about the mechanics linking K^+ and voltage in gating of TOK1. For the Shaker K^+ channel, voltage drives conformational changes of the S4 voltage sensors through two distinct steps, only the latter of which occurs co-operatively [10]. For the interaction that we have identified, it is plausible that this too appears only late in relation to K^+ binding. We note that, to date, all mutants identified to affect the K^+-sensitivity of TOK1 fall into two groups, the first group affecting only the high-affinity response and the second affecting both K^+-dependencies. None have been identified to date that affect only the (low-affinity) K^+-sensitivity of TOK1 conductance. Thus it is possible to envision a structure in which two K^+-binding pockets occur in series, with access to the second, deeper (high-affinity), site via the first, and cross-domain interactions reflecting the occupation of both sites. It will be of interest now to determine the mechanism of this interaction, whether it depends on intra- or inter-polypeptide associations in the functional channel, and its relationship to internal conformational changes [22,49] that also contribute to the K^+-sensitivity of this channel.

In conclusion, we have identified in the first pore domain of the yeast K^+ channel TOK1 a key residue that is critical to determining the characteristics of K^+-dependent gating. The site appears to demarcate two K^+-sensitive gating domains at the extracellular surface of the protein. Its mutation affects the apparent affinity for, and in the extreme also the sign of, the gating response to extracellular K^+, but has no effect on TOK1 permeation, indicating that K^+ binding for gating and permeation occur at distinct sites. We also offer primary evidence for a synergy in K^+-dependent gating between the two pore domains of TOK1 that must translate over distances in excess of 20 Å across the mouth of the pore. These findings indicate a remarkable integration of gating and its K^+ sensitivity within the structure of TOK1.

We are grateful to Dr Ingo Dreyer (Golm, Germany) for his suggestions early in the preparation of this manuscript and to Mr Adrian Hills for his help in software development for data analysis. This work was supported by the UK Biotechnology and Biological Sciences Research Council grants 17/C13599, BB/D001528/1 and 17/P13610 to M. R. B. and by a Life Science Fellowship 'Ausländische Wissenshaftler für Brandenburg' of the Biotechologie Stiftung Berlin-Brandenburg and a Royal Society of Edinburgh travel grant to I. J.

REFERENCES

1 Hille, B. (2001) Ionic Channels of Excitable Membranes, Sinauer Press, Sunderland, MA
2 Lesage, F., Guillemare, E., Fink, M., Duprat, F., Lazdunski, M., Romey, G. and Barhanin, J. (1996) TWIK-1, a ubiquitous human weakly inward rectifying K^+ channel with a novel structure. EMBO J. **15**, 1004–1011
3 Czempinski, K., Zimmermann, S., Ehrhardt, T. and Müller-Röber, B. (1997) New structure and function in plant K^+ channels: KCO1, an outward rectifier with a steep Ca^{2+} dependency. EMBO J. **16**, 2565–2575
4 Long, S. B., Campbell, E. B. and MacKinnon, R. (2005) Crystal structure of a mammalian voltage-dependent Shaker family K^+ channel. Science **309**, 897–903
5 Long, S. B., Campbell, E. B. and MacKinnon, R. (2005) Voltage sensor of Kv1.2: structural basis of electromechanical coupling. Science **309**, 903–908
6 Jiang, Y. X., Lee, A., Chen, J. Y., Ruta, V., Cadene, M., Chait, B. T. and MacKinnon, R. (2003) X-ray structure of a voltage-dependent K^+ channel. Nature (London) **423**, 33–41
7 Jiang, Y. X., Lee, A., Chen, J. Y., Cadene, M., Chait, B. T. and MacKinnon, R. (2002) Crystal structure and mechanism of a calcium-gated potassium channel. Nature (London) **417**, 515–522
8 Doyle, D. A., Cabral, J. M., Pfuetzner, R. A., Kuo, A. L., Gulbis, J. M., Cohen, S. L., Chait, B. T. and MacKinnon, R. (1998) The structure of the potassium channel: molecular basis of K^+ conduction and selectivity. Science **280**, 69–77
9 Mannuzzu, L. M. and Isacoff, E. Y. (2000) Independence and cooperativity in rearrangements of a potassium channel voltage sensor revealed by single subunit fluorescence. J. Gen. Physiol. **115**, 257–268
10 Pathak, M., Kurtz, L., Tombola, F. and Isacoff, E. (2005) The cooperative voltage sensor motion that gates a potassium channel. J. Gen. Physiol. **125**, 57–69
11 Gonzalez, C., Morera, F. J., Rosenmann, E., Alvarez, O. and Latorre, R. (2005) S3b amino acid residues do not shuttle across the bilayer in voltage-dependent Shaker K^+ channels. Proc. Natl. Acad. Sci. U.S.A. **102**, 5020–5025
12 Mannikko, R., Elinder, F. and Larsson, H. P. (2002) Voltage-sensing mechanism is conserved among ion channels gated by opposite voltages. Nature (London) **419**, 837–841
13 Sesti, F., Rajan, S., Gonzalez-Colaso, R., Nikolaeva, N. and Goldstein, S. A. N. (2003) Hyperpolarization moves S4 sensors inward to open MVP, a methanococcal voltage-gated potassium channel. Nat. Neurosci. **6**, 353–361
14 Latorre, R., Olcese, R., Basso, C., Gonzalez, C., Munoz, F., Cosmellli, D. and Alvarez, O. (2003) Molecular coupling between voltage sensor and pore opening in the *Arabidopsis* inward rectifier K^+ channel KAT1. J. Gen. Physiol. **122**, 459–469
15 Ketchum, K. A., Joiner, W. J., Sellers, A. J., Kaczmarek, L. K. and Goldstein, S. A. N. (1995) A new family of outwardly rectifying potassium channel proteins with 2 pore domains in tandem. Nature (London) **376**, 690–695
16 Zhou, X. L., Vaillant, B., Loukin, S. H., Kung, C. and Saimi, Y. (1995) YKC1 encodes the depolarization-activated K^+ channel in the plasma membrane of yeast. FEBS Lett. **373**, 170–176
17 Lesage, F., Guillemare, E., Fink, M., Duprat, F., Lazdunski, M., Romey, G. and Barhanin, J. (1996) A pH-sensitive yeast outward rectifier K^+ channel with two pore domains and novel gating properties. J. Biol. Chem. **271**, 4183–4187
18 Vergani, P., Miosga, T., Jarvis, S. M. and Blatt, M. R. (1997) Extracellular K^+ and Ba^{2+} mediate voltage-dependent inactivation of the outward-rectifying K^+ channel encoded by the yeast gene *TOK1*. FEBS Lett. **405**, 337–344
19 Vergani, P., Hamilton, D., Jarvis, S. and Blatt, M. R. (1998) Mutations in the pore regions of the yeast K^+ channel YKC1 affect gating by extracellular K^+. EMBO J. **17**, 7190–7198
20 Saldana, C., Naranjo, D., Coria, R., Pena, A. and Vaca, L. (2002) Splitting the two pore domains from TOK1 results in two cationic channels with novel functional properties. J. Biol. Chem. **277**, 4797–4805
21 Vergani, P. and Blatt, M. R. (1999) Mutations in the yeast two pore K^+ channel YKC1 identify functional differences between the pore domains. FEBS Lett. **458**, 285–291
22 Loukin, S. H. and Saimi, Y. (1999) K^+-dependent composite gating of the yeast K^+ channel, Tok1. Biophys. J. **77**, 3060–3070
23 Jiang, Y. X., Lee, A., Chen, J. Y., Cadene, M., Chait, B. T. and MacKinnon, R. (2002) The open pore conformation of potassium channels. Nature (London) **417**, 523–526
24 Higuchi, R. (1990) Recombinant PCR. In PCR Protocols (Innis, M. A., Gelfand, D. H., Sninsky, J. J. and White, T. J., eds.), pp. 177–196, Academic Press, London
25 Hill, A. V. (1910) The possible effects of the aggregation of the molecules of hemoglobin on its dissociation curves. J. Physiol. **40**, 4–7
26 Bertl, A., Bihler, H., Reid, J. D., Kettner, C. and Slayman, C. L. (1998) Physiological characterization of the yeast plasma membrane outward rectifying K^+ channel, DUK1 (TOK1), *in situ*. J. Membr. Biol. **162**, 67–80
27 LiCata, V. J. and Ackers, G. K. (1995) Long-range small magnitude non-additivity of mutational effects in proteins. Biochemistry **34**, 3133–3139
28 Loukin, S. H. and Saimi, Y. (2002) Carboxyl tail prevents yeast K^+ channel closure: proposal of an integrated model of TOK1 gating. Biophys. J. **82**, 781–792
29 Schwede, T., Kopp, J., Guex, N. and Peitsch, M. C. (2003) SWISS-MODEL: an automated protein homology-modeling server. Nucleic Acids Res. **31**, 3381–3385
30 Guex, N. and Peitsch, M. C. (1997) SWISS-MODEL and the Swiss-PdbViewer: an environment for comparative protein modeling. Electrophoresis **18**, 2714–2723
31 Peitsch, M. C. (1995) Protein modelling by email. Biotechnology **13**, 658–660
32 Baukrowitz, T. and Yellen, G. (1996) Use-dependent blockers and exit rate of the last ion from the multiion pore of a K^+ channel. Science **271**, 653–656
33 Kiss, L. and Korn, S. J. (1998) Modulation of C-type inactivation by K^+ at the potassium channel selectivity filter. Biophys. J. **74**, 1840–1849
34 Melishchuk, A., Loboda, A. and Armstrong, C. M. (1998) Loss of Shaker K^+ channel conductance in 0 K^+ solutions: role of the voltage sensor. Biophys. J. **75**, 1828–1835
35 Geiger, D., Becker, D., Lacombe, B. and Hedrich, R. (2002) Outer pore residues control the H^+ and K^+ sensitivity of the *Arabidopsis* potassium channel AKT3. Plant Cell **14**, 1859–1868
36 Lopez-Barneo, J., Hoshi, T., Heinemann, S. H. and Aldrich, R. W. (1993) Effects of external cations and mutations in the pore region on C-type inactivation of Shaker potassium channels. Recept. Channels **1**, 61–71
37 Doi, T., Fakler, B., Schultz, J. H., Schulte, U., Brandle, U., Weidemann, S., Zenner, H. P., Lang, F. and Ruppersberg, J. P. (1996) Extracellular K^+ and intracellular pH allosterically regulate renal $K_{if}1.1$ channels. J. Biol. Chem. **271**, 17261–17266
38 Schulte, U., Weidemann, S., Ludwig, J., Ruppersberg, J. P. and Fakler, B. (2001) K^+-dependent gating of $K_{if}1.1$ channels is linked to pH gating through a conformational change in the pore. J. Physiol. **534**, 49–58
39 Sackin, H., Vasilyev, A., Palmer, L. G. and Krambis, M. (2003) Permeant cations and blockers modulate pH gating of ROMK channels. Biophys. J. **84**, 910–921
40 Dahlmann, A., Li, M., Gao, Z. H., McGarrigle, D., Sackin, H. and Palmer, L. G. (2004) Regulation of K_{if} channels by intracellular pH and extracellular K^+: mechanisms of coupling. J. Gen. Physiol. **123**, 441–454
41 Ache, P., Becker, D., Ivashikina, N., Dietrich, P., Roelfsema, M. R. G. and Hedrich, R. (2000) GORK, a delayed outward rectifier expressed in guard cells of *Arabidopsis thaliana*, is a K^+-selective, K^+-sensing ion channel. FEBS Lett. **486**, 93–98
42 Gaymard, F., Pilot, G., Lacombe, B., Bouchez, D., Bruneau, D., Boucherez, J., Michaux-Ferriere, N., Thibaud, J. B. and Sentenac, H. (1998) Identification and disruption of a plant shaker-like outward channel involved in K^+ release into the xylem sap. Cell **94**, 647–655
43 Blatt, M. R. (1988) Potassium-dependent bipolar gating of potassium channels in guard cells. J. Membr. Biol. **102**, 235–246
44 Schroeder, J. I. (1989) Quantitative analysis of outward rectifying K^+ channel currents in guard cell protoplasts from *Vicia faba*. J. Membr. Biol. **107**, 229–235
45 Blatt, M. R. and Gradmann, D. (1997) K^+-sensitive gating of the K^+ outward rectifier in *Vicia* guard cells. J. Membr. Biol. **158**, 241–256
46 Roelfsema, M. R. G. and Prins, H. B. A. (1997) Ion channels in guard cells of *Arabidopsis thaliana* (L.) Heynh. Planta **202**, 18–27
47 Johansson, I., Wulfetange, K., Poree, F., Michard, E., Lacombe, B., Sentenac, H., Thibaud, J.-P., Mueller-Roeber, B., Blatt, M. R. and Dreyer, I. (2006) K^+ dependence of the *Arabidopsis* K^+ channel SKOR implicates a mechanism of gating coupled to ion permeation. Plant J., in the press
48 Smith-Maxwell, C. J., Ledwell, J. L. and Aldrich, R. W. (1998) Role of the S4 in cooperativity of voltage-dependent potassium channel activation. J. Gen. Physiol. **111**, 399–420
49 Loukin, S. H., Lin, J. Y., Athar, U., Palmer, C. and Saimi, Y. (2002) The carboxyl tail forms a discrete functional domain that blocks closure of the yeast K^+ channel. Proc. Natl. Acad. Sci. U.S.A. **99**, 1926–1930
50 Creighton, T. E. (1993) Proteins, pp. 1–507, Freeman, New York

Received 23 August 2005/15 November 2005; accepted 16 November 2005
Published as BJ Immediate Publication 16 November 2005, doi:10.1042/BJ20051380